Published in final edited form as:
Mol Pharm. 2010 February 1; 7(1): 86. doi:10.1021/mp900138a.

Partial Correction of Cystic Fibrosis Defects with PLGA Nanoparticles Encapsulating Curcumin

Malgorzata S. Cartiera[1], **Elisa C. Ferreira**[2], **Christina Caputo**[2], **Marie E. Egan**[2,3], **Michael J. Caplan**[3], and **W. Mark Saltzman**[*]

[1] Yale University, Department of Biomedical Engineering, New Haven, CT 06520-8260

[2] Yale University, School of Medicine, Department of Pediatrics, New Haven, CT 06510-3206

[3] Yale University, School of Medicine, Department of Cell and Molecular Physiology, New Haven, CT 06510-3206

Abstract

Cystic fibrosis (CF) is a common life threatening genetic disease (incidence: ~1 in 2500 live births). CF is caused by mutations in CFTR, a chloride channel involved in epithelial secretion of fluid and electrolytes. The most common mutation entails the deletion of a phenylalanine in position 508 that causes protein misfolding and abnormal CFTR processing. The ΔF508 mutation accounts for approximately 70% of all CF alleles and about 90% of CF patients carry at least one copy of ΔF508 CFTR. Curcumin, a natural constituent of *Curcuma Longa* (turmeric spice), is a non-toxic low-affinity SERCA (Sarco (Endo)plasmic Reticulum Calcium ATPase) pump inhibitor thought to permit ΔF508 CFTR escape from the ER. The compound has been shown to be capable of correcting the defect in cell lines and mice expressing ΔF508 CFTR. In this work, poly-lactic-co-glycolic acid (PLGA) nanoparticles encapsulating curcumin were synthesized and used to treat two different CF mouse strains in an effort to correct the defects associated with CF by improving bioavailability of the compound, which has previously been a challenge in treatment with curcumin. Our results suggest that oral administration of PLGA nanoparticles encapsulating curcumin enhances the effects of curcumin therapy in CF mice, as compared to delivery of non-encapsulated curcumin.

Keywords

Nanoparticle; Curcumin; Cystic Fibrosis; PLGA; Nasal Potential Difference

INTRODUCTION

Cystic fibrosis (CF) is an autosomal recessive disease that affects 1 in 2500 live births with the most common mutation involving a deletion of the phenylalanine residue at position 508[1]. The ΔF508 mutation accounts for 70% of all CF alleles and 90% of CF patients carry at least one copy of ΔF508 CFTR [1, 2]. The mutation disrupts biosynthetic processing of CFTR so that the protein is misfolded resulting in rapid degradation of the CFTR protein in a pre-Golgi and lysosome-independent compartment [3]. Even though ΔF508 CFTR is able to function as a cAMP-gated chloride channel, it can not reach the apical plasma membranes of airway, pancreatic, and intestinal epithelial cells and consequently, salt and water secretion by epithelia is compromised [1, 4]. Those affected by CF often suffer from respiratory infections, obstruction

*Department of Biomedical Engineering, MEC 414, Yale University, 55 Prospect St, New Haven, CT 06511, Phone: (203) 432 - 4262, Fax: (203) 432 - 0030, mark.saltzman@yale.edu.

of the airways by thick viscous mucous, pancreatic exocrine insufficiency, cirrhosis of the liver, and infertility. Recent studies suggest that the CF phenotype could be at least partially alleviated if the mutant CFTR protein could be induced to relocate from the endoplasmic reticulum (ER) to the plasma membrane [2, 5].

Curcumin (diferuloylmethane), a hydrophobic compound, is a low molecular weight dietary polyphenolic shown to have antioxidant, antiviral, anti-infectious and anti-carcinogenic effects [6–11]. It is a natural constituent of *Curcuma Longa* (turmeric spice) and is considered a non-toxic, low-affinity SERCA pump inhibitor [12]. In cell lines and mice expressing the ΔF508 CFTR mutation, the compound has been shown capable of at least partially correcting phenotypic defects [13]. Different mechanisms of action for curcumin have been proposed. One mechanism postulates that curcumin lowers calcium levels in the ER, thereby causing inhibition of calcium-binding chaperones that entrap the misfolded CFTR thus allowing CFTR to escape and reach the cell surface to perform its function [5, 14]. Others speculate that curcumin may modulate the function of more than one transport protein in the cell and might bind to Na, K-ATPase from the extracellular side[11] or that its action is due to a more local effect on surface resident ΔF508-CFTR channels, where curcumin acts as a modulator of CFTR gating that strongly activates mutant channels that otherwise cannot be opened by the normal ATP-dependent mode of gating [15].

Studies in CF mice using free curcumin have shown that curcumin is capable of correcting defects associated with the disease [13], but it has also been observed that some strains do not respond to curcumin treatment [16–19]. One possible explanation for the conflicting results *in vivo* is differing levels of bioavailability across strains. If this were true, curcumin would be similar to many orally delivered drugs: it has been estimated that roughly 40% of all investigational compounds fail development because of poor bioavailability [20]. Clinical studies confirm curcumin's poor absorption and rapid metabolism [6, 21, 22]. In an effort to improve bioavailability and provide more consistent biological effects across species strains, nanoparticles (NPs) encapsulating curcumin were tested *in vivo*. Our goal was to synthesize biodegradable curcumin particles that were able to (1) effectively correct defects associated with CF and (2) improve bioavailability of the compound *in vivo* across species strains.

METHODS AND MATERIALS

Nanoparticle Preparation

Materials—50:50 PLGA (poly-lactic-co-glycolic acid), M_W = 30–70 kDa with an inherent viscosity of 0.59 dL/g, was supplied by Birmingham Polymers Inc. (Birmingham, AL). Polyvinyl alcohol (PVA), M_W = 12–23 kDa; 87–89% hydrolyzed, and curcumin were obtained from Sigma-Aldrich (St. Louis, MO). Ethyl acetate and all other reagents used were supplied by Fisher Scientific (Fairlawn, NJ).

NP Preparation—Nanoparticles were prepared using a single-emulsion technique [23, 24]. The method is ideal for encapsulation of hydrophobic compounds and is sometimes referred to as the 'solvent-evaporation' method. Briefly, two hundred milligrams of PLGA polymer was dissolved in 2 ml of ethyl acetate solvent in a glass tube. Twenty milligrams of curcumin powder was added to the polymer/solvent mixture and allowed 30 minutes to dissolve, with intermittent vortexing. Four milliliters of an aqueous 5% w/v solution of PVA was poured into a glass tube. While vortexing the surfactant solution at a high setting, the solvent mixture was added dropwise. Once all of the drug/polymer mixture was added to the PVA solution, the contents were vortexed for an additional 10 seconds at a high setting. The tube contents were then sonicated for 3×10 seconds at 38% amplitude with a TMX 400 sonic disruptor (Tekmar, Cincinnati, OH) to create an oil-in-water emulsion. Immediately after sonication, the emulsion was poured into 100 ml of an aqueous 0.3% w/v PVA solution under rapid stirring with a

magnetic stirrer. The resulting nano-sized particles were stirred in the solution for 3 hours to allow for ethyl acetate evaporation. The particles were then collected by centrifugation, washed 3 times with Milli-Q treated water, and finally resuspended in 4 ml of Milli-Q treated water and dried on a lyophilizer. Long-term storage was in an airtight container at −20°C.

NP Characterization

The morphology, percent loading, and kinetics of drug release were evaluated following synthesis of the particles.

Morphology—Nanoparticles were fixed to aluminum sample stubs with double-sided carbon tape and sputter coated with gold for viewing by scanning electron microscopy. A scanning electron microscope (SEM; XL30 ESEM, FEI Company) was used to assess the particle surface properties. Micrographs were analyzed with NIH SCION imaging software (Scion Corporation, Frederick MD) to determine particle size distribution.

Loading and Release Profile—Fluorescence techniques were used to evaluate the actual amount of drug encapsulated in the particles and the release profile of the compound. Because curcumin has inherent fluorescent properties (excitation/emission = 365 nm/450 nm), spectroscopy (SpectraMax, Molecular Devices) was used to generate a calibration curve of fluorescence values at known concentrations for the compound that allowed quantification of the percent loading of the drug and the controlled-release profile for the spheres encapsulating drug.

For characterizing the release profile of curcumin nanoparticles, a known quantity of the particles was suspended in Dulbecco's Phosphate Buffered Saline (PBS) in a glass container and incubated at 37°C, 100 rpm in a rotary shaker. Samples of the supernatant were collected at designated time points and analyzed using spectroscopy (λ = 430nm). In determining the amount of compound encapsulated in the particles, a known quantity of curcumin nanoparticles was dissolved in 1 ml of dimethyl sulfoxide (DMSO) overnight. The sample was centrifuged at 10,000 rpm for 5 minutes followed by collection and spectroscopic analysis of the supernatant.

In Vivo Experiments

Nasal Potential Difference (NPD) Measurement—Gene-targeted mice homozygous for the 3F508 mutation on either 129 or C57/BL6 backgrounds were used in the study. Heterozygous mice of both strains were included as controls.

The general *in vivo* study design followed that of Egan et al., where NPD measurement details have been described previously [13]. Briefly, NPD measurement involved placing a probing electrode into one nostril of the mouse, while a reference electrode (27 gauge butterfly needle filled with 4% agar in Ringer's solution) was inserted subcutaneously. A microperfusion pump controlled the flow of solution through the probing electrode at 0.2 ml/hour. Mice were anesthetized with ketamine/xylazine and saline drops maintained moistened eyes. Subjects were placed on a warming pad to preserve body temperature and were continually monitored throughout the duration and following the procedure.

NPD measurements commenced with a control Ringer's solution. The perfusion solution was then changed to a Ringer's solution containing 100 μM amiloride, followed by a chloride-free solution with amiloride, and finally a chloride-free solution containing 10 μM isoproterenol. The tracings recorded represent the full time course of the NPD measurement (average time course was approximately 30 minutes).

Subjects in each group had baseline NPD measurements taken prior to treatment initiation. Following baseline measurement, each mouse was orally administered (1) free curcumin: total of 3.75 mg, (2) non-drug loaded NPs (blank vehicle control), (3) curcumin NPs at a low-dose: total curcumin encapsulated amount equivalent to 3.75 mg, and (4) curcumin NPs at a high-dose: curcumin amount released from nanoparticles at Day 4 equivalent to 3.75 mg. All treatments were dissolved/suspended in Peptamen®, a peptide-based liquid formula manufactured by Nestlé Nutrition and administered 3 times daily over a three day period with NPD measurement taken on Day 4. Mice were provided a minimum 2 week recovery period between treatment options to allow for clearance of anesthetic and curcumin effects associated with prior treatment (Figure 4). At the conclusion of the study, animals were sacrificed following a typical dosing schedule with one of the above detailed treatment options, and blood and tissue samples were collected for analysis. All procedures were approved by the Yale Institutional Animal Care and Use Committee.

Nasal potential difference data was analyzed in the following manner:

The *Isoproterenol Response (IR)* was calculated for baseline and treatment NPDs. IR was calculated by subtracting the average Low Chloride Amiloride response from the average Low Chloride Amiloride Isoproterenol response.

Treatment IR values were compared to baseline IR values to determine a ‘delta IR value. A difference greater than 2 mV between baseline and treatment IR values was considered a full response.

To determine the *Amiloride-Isoproterenol Response (AIR)*, the average Ringers Amiloride response was subtracted from the average Low Chloride Amiloride Isoproterenol response. Treatment AIR values were then compared with baseline AIR values to arrive at a ‘delta AIR’ value.

Serum and Tissue Analysis—Five hundred microliters of blood was collected from each animal (post-treatment) and placed in a centrifuge tube with heparin. Samples were centrifuged for 10 minutes at 4300 rpm. The serum layer was carefully collected into another centrifuge tube and stored at −80°C to await LC/MS/MS analysis. The LC/MS/MS instrumentation consisted of an Agilent HPLC system (1100 series, USA) and a Micromass Quattro micro™ triple quadrupole mass spectrometer, inclusive of the HPLC unit controlled by Micromass Masslynx® software Version 3.5. The analytical column C18 (Life Science, 30 mm × 2.1 mm) was used. The mobile phase was a mixture of acetonitrile/water with 0.1% formic acid and the internal standard used was reserpine. The injection volume was 50 μL with flow rate set at 0.3 ml/min. Curcumin detection was found to be linear within a range of 50–1000 ng/mL, with a limit of detection of 5 ng/mL.

The nasal epithelium, lung, gut (i.e., ileum, jejunum, and duodenum), spleen, liver and kidney were harvested from each animal, rinsed in cold PBS and fixed in 3.7% formaldehyde for 24 hours. Tissues were then placed in 70% ethanol, followed by paraffin embedding. Five-micron thick tissue sections taken from the center of each paraffin-embedded tissue were stained with haematoxylin and eosin and viewed using bright field and fluorescent microscopy at 60 times magnification (Olympus IX71, Olympus).

Data Analysis—Following collection of NPD data for all animals, the Isoproterenol Response (IR) and Amiloride-Isoproterenol Response (AIR) values were averaged and analyzed. Groups included (1) free curcumin, (2) non-drug loaded NPs (blank vehicle control), and (3) curcumin NPs – greatest response from either low-dose or high-dose treatment.

Representative individual IR mouse response data is shown in Figure 5 for subjects from each of the CF strains.

Statistical comparisons between groups were carried out using analysis of variance (ANOVA) and Tukey analysis for multiple comparisons. A difference was considered significant when $P<0.05$. In the data presented (Figures 6 and 7), the values represent the average with error bars representing one standard error of the mean, n=7. Data were plotted and statistical analysis was carried out using GraphPad software.

RESULTS

Curcumin Nanoparticles

Representative scanning electron micrographs illustrate that curcumin-loaded PLGA particles have a characteristic round shape and are monodisperse (Figure 1), with a mean diameter of 77 nm and standard deviation of 16 nm. Curcumin particles have an average drug loading of 7.6% w/w which represents an encapsulation efficiency of 76%. The rate of curcumin release from NPs has a biphasic nature, where an initial burst release was seen during the first several hours followed by a sustained, more uniform release lasting over 19 days (Figure 2). The burst effect, with a time constant of 0.11, is most likely caused by poorly entrapped drug or drug adsorbed onto the outer surface of the particles [25].

In Vivo Work

NPD Measurement—Two different CF mouse strains were treated with curcumin NPs to test the hypothesis that nanoencapsulation of curcumin would improve therapeutic function and bioavailability of the compound. The nasal potential difference (NPD) was measured in mice since the nasal epithelium is easily accessible and capable of demonstrating the CF bioelectric defects [26]. *In vivo* measurement assesses the voltage across the epithelium and correlates to the transport of sodium and chloride across cell membranes. In clinical practice, it is used as a diagnostic tool to determine the efficacy of treatments in CF patients [27].

NPD measurement involved bathing the nasal epithelium with different solutions while voltage measurements recorded electrochemical responses. The procedure started with a Ringers solution that served as a control fluid followed by a Ringers-Amiloride solution. The addition of amiloride, a sodium channel blocker, allows measurement of sodium absorption. Sodium absorption is pathologically increased in the absence of functional CFTR due to the loss of the inhibitory effect of the CFTR protein on the activity of the epithelial sodium channel (ENaC). The third solution introduced involved a low chloride solution in the presence of amiloride, which is intended to produce a large electrochemical gradient favoring chloride secretion via efflux through all open chloride channels. The final solution added is a Low Chloride-Amiloride-Isoproterenol mixture. Isoproterenol, a β-agonist that leads to the elevation of cAMP, induces activation of CFTR which is a cAMP stimulated chloride channel. While in normal subjects isoproterenol elicits cAMP-regulated chloride secretion, this response is blunted or absent in CF-affected patients and animal models [26]. Representative NPD data for a typical heterozygote and CF mouse are depicted in Figure 3.

A treatment in CF mice is deemed ‘favorable’ when the NPD mimics a tracing typical for that of a heterozygous or wild-type mouse, particularly when NPD values become more negative following isoproterenol administration. Moreover, an animal is considered to have a full response if the difference between baseline and treatment is larger than 2 mV. Data presented in Figure 6 provides average deltaIR values for 129 mixed background and C57/BL6 mouse strains. Both strains exhibit a hyperpolarization to nanoparticle treatment with 129 mixed background mice having a statistically significant response when compared to free curcumin

treatment. NPD data were also analyzed against more demanding criteria that focused on the amiloride-isoproterenol response (Figure 7). Even when examined in the context of this more stringent criterion, the same trend was seen where curcumin NP treatment demonstrated improved effectiveness over free curcumin. It is important to note that although no statistical difference was observed in C57/BL6 mice, a majority of the animals did have a greater than 2 mV change indicating a full response when treated with curcumin nanoparticles.

Serum and Tissue Analysis—Blood serum samples were analyzed by BRI Biopharmaceutical Research Inc. (Vancouver, BC) using LC/MS/MS. The evaluation included generating a calibration curve for curcumin in mouse serum (Figure 8), examining quality control samples, as well as subsequent analysis of experimental blood serum samples from animals included in the *in vivo* study. Resultant data showed no detectable levels of curcumin in the serum of mice in either strain group, across treatment options. It is important to note, however, that curcumin metabolites were not examined in this study.

Tissues collected from animals post-treatment were analyzed using microscopy to discern gross morphological changes associated with curcumin NP treatment. In the rodent model of cystic fibrosis, the most dramatic histopathological changes seen are in the crypts of Lieberkuhn, following a proximal to distal gradient of severity with mildest changes affecting the duodenum and the most extreme affecting the ileum and the colon [1, 4]. For this reason, microscopic analysis focused on the ileum and the colon. Typical histology for a heterozygote and CF-affected mouse was observed in the tissues, with an intact epithelium where the lumen was free of necrotic material, no noticeable distention of crypts or increase in the number of goblet cells in the villi/crypts. Since no dramatic morphological changes were detected when comparing untreated CF tissue with nanoparticle treated CF tissue, we conclude that NPs do not have a toxic affect at the tissue level (Figure 9).

DISCUSSION

Curcumin has shown to exhibit antioxidant, anti-inflammatory, antimicrobial, and anticarcinogenic activities and the hepato- and nephro-protective, thrombosis suppressing, myocardial infarction protective, hypoglycemic, and anti-rheumatic effects of curcumin are well established [6–10]. In addition, various animal models and human studies have demonstrated that curcumin is extremely safe even at very high doses [8, 9, 21, 28] but despite its safety and potential for treatment/prevention of a wide variety of human diseases, free curcumin has a poor absorption and rapid metabolism that limit its bioavailability *in vivo* [22].

Delivery technologies, such as nanoparticles, promise to improve drug delivery in several situations: poor permeability of the drug through cell membranes, low accessibility of the drug to its site of action within the cell, degradation of the drug in specific cell compartments, or toxicity due to unintended exposure of cells or cellular compartments [29]. Oral delivery of compounds using polymer particles has previously shown to improve absorption and is thought to be the result of the nanoparticles' physicochemical characteristics, which protect the contents against degradation in the gastrointestinal tract and facilitate uptake of the compound (associated or not associated to the nanoparticles) through a paracellular or a transcellular pathway [30, 31]. It has been suggested that encapsulation of curcumin in a polymer or lipid vehicle could overcome many of the bioavailability issues associated with curcumin [6, 22, 32, 33] and improve delivery of the compound to secretory epithelial cells affected by the CF defect, resulting in enhanced alleviation of aspects of the CF phenotype. The experiments described in this study evaluated PLGA nanoparticles encapsulating curcumin to treat cystic fibrosis.

Nanoparticles were prepared using methods and materials that yielded particles appropriate for oral delivery. The single emulsion method employed PLGA, PVA, and ethyl acetate which

produced biodegradable particles capable of sustained compound release with a homogeneous size less than 200 nm and bioadhesive properties [24, 34, 35]. PLGA is a widely used biodegradable polymer and has shown to have bioadhesive properties that facilitate its binding with the mucosa of the GI tract [36], while use of PVA results in spheres that are relatively uniform, small in size, and easily redispersed in aqueous medium [29]. Ethyl acetate was the solvent of choice in these experiments as it has been shown to produce smaller particles [37] and it provided improved dissolution of curcumin when compared to other solvents tested.

PLGA nanoparticles were loaded with high levels of curcumin in an optimal size range. Fabricated particles had a mean diameter of 77 nm (range of 50 nm-120 nm) and encapsulated the hydrophobic compound, curcumin, at a loading of 7.6%. Release of the compound from the biodegradable NPs was maintained over an extended period in a controlled fashion. An initial burst was observed during the first 24 hours, where approximately 20% of the particle contents are released followed by a more sustained profile where an average of 1.4 μg of curcumin was released per day.

Upon oral administration of curcumin nanoparticles to mice possessing the CF phenotype, we observed a change in the electrophysiological phenotype in animals treated with curcumin nanoparticles. Mice belonging to the 129 background colony demonstrated an average isoproterenol response of 5.0 mV with curcumin NP treatment, as compared to a mean response of 0.4 mV with free curcumin. In C57/BL6 mice, an average change of 3.7 mV was seen with curcumin NP treatment, as opposed to 0.4 mV with the free compound. When NPD data was evaluated against more demanding criterion that evaluated the amiloride-isoproterenol response, curcumin NP treatment still demonstrated superior effectiveness over free curcumin. A response to blank NPs was observed in a small number of animals and although precautions were taken to allow prior treatment clearance, it is hypothesized that this effect may be attributed to residual curcumin NPs deposited during prior applications of the treatment regimens.

Tissue and serum analysis conducted in this study did not reveal the pharmacokinetic distribution of free curcumin or curcumin nanoparticles; however previous experiments evaluating free curcumin serum levels in mice showed that the compound could only be detected at extremely high doses in the range of 300 mg/kg: even at these high doses, curcumin was only measured at the nanogram/picogram level [22, 38]. The main reason for low levels of curcumin in the serum is thought to be due to extensive reduction, most likely through alcohol dehydrogenase followed by conjugation. Previous work has suggested that the presence of conjugative enzyme activities for glucuronidation and sulfation of curcumin in the liver, kidney and intestinal mucosa are evidence that orally administered curcumin is likely absorbed from the alimentary tract and present in the general blood circulation only after largely being metabolized to the form of glucuronide and sulfate conjugates [22]. Our analysis did not include evaluation of curcumin metabolites; however should future work with curcumin nanoparticles be conducted, it is strongly recommended that metabolite detection be incorporated into the study.

The NPD data from this study supports the hypothesis that nanoparticles can improve the therapeutic efficacy of orally delivered curcumin. We believe that the nanoparticles provide protection against drug degradation and propose that the particles traverse the gut epithelium, gain systemic access and arrive at tissues or intracellular locations that are highly relevant for therapy. In other work, using human bronchial epithelial cells to investigate the intracellular fate of NPs, we have observed that particles co-localize to a large extent with the Golgi and possibly, the ER [39] and anticipate that the administered curcumin nanoparticles were trafficked to these organelles after systemic distribution. One of the proposed mechanisms of action for curcumin in CF suggests that curcumin may act by lowering calcium levels in the ER [14]. If

this is accurate, delivery of curcumin-containing NPs to the ER and ER-associated organelles may increase the local availability of this compound at or near its site of functional activity. An alternate mechanism of curcumin action suggests that curcumin's positive effects are due to local effects it exerts on the gating properties of surface resident ΔF508-CFTR channels [15]. However, because we were unable to detect curcumin in blood, it is not clear whether the nanoparticles gain systemic access or if they accumulate in the intestines and tissues where they slowly release drug. Nevertheless, particle encapsulation of curcumin may provide an avenue through which higher levels of curcumin are able to survive the harsh environment of the gut and reach relevant tissues to exert these potentially beneficial local effects.

CONCLUSIONS

PLGA nanoparticles encapsulating curcumin enhance the capacity of curcumin to partially correct at least a subset of CF symptoms *in vivo*, both in 129 background and C57/BL6 mouse strains. Analysis of NPD data establishes that treatment of mice with curcumin nanoparticles elicits a more favorable response over free drug in both strains.

Acknowledgments

This work was supported by grants from NIH RO1-EB00487 to WMS, NIH R01-DK053428 and CFF EGAN04G0 to MEE, and NIH grants AI-066-738 and DK072612 to MJC.

References

1. Snouwaert JN, Brigman KK, Latour AM, Malouf NN, Boucher RC, Smithies O, Koller BH. An animal model for cystic fibrosis made by gene targeting. Science 1992;257(5073):1083–1083. [PubMed: 1380723]
2. Sharma M, Benharouga M, Hu W, Lukacs GL. Conformational and temperature-sensitive stability defects of the delta F508 cystic fibrosis transmembrane conductance regulator in post-endoplasmic reticulum compartments. J Biol Chem 2001;276(12):8942–8942. [PubMed: 11124952]
3. Skach WR. Defects in processing and trafficking of the cystic fibrosis transmembrane conductance regulator. Kidney Int 2000;57(3):825–825. [PubMed: 10720935]
4. Zeiher BG, Eichwald E, Zabner J, Smith JJ, Puga AP, McCray PB Jr, Capecchi MR, Welsh MJ, Thomas KR. A mouse model for the delta F508 allele of cystic fibrosis. J Clin Invest 1995;96(4):2051–2051. [PubMed: 7560099]
5. Egan ME, Glockner-Pagel J, Ambrose C, Cahill PA, Pappoe L, Balamuth N, Cho E, Canny S, Wagner CA, Geibel J, Caplan MJ. Calcium-pump inhibitors induce functional surface expression of Delta F508-CFTR protein in cystic fibrosis epithelial cells. Nat Med 2002;8(5):485–485. [PubMed: 11984593]
6. Hsu CH, Cheng AL. Clinical studies with curcumin. Adv Exp Med Biol 2007;595:471–80. [PubMed: 17569225]
7. Lao CD, Demierre MF, Sondak VK. Targeting events in melanoma carcinogenesis for the prevention of melanoma. Expert Rev Anticancer Ther 2006;6(11):1559–1559. [PubMed: 17134361]
8. Sharma RA, McLelland HR, Hill KA, Ireson CR, Euden SA, Manson MM, Pirmohamed M, Marnett LJ, Gescher AJ, Steward WP. Pharmacodynamic and pharmacokinetic study of oral Curcuma extract in patients with colorectal cancer. Clin Cancer Res 2001;7(7):1894–1894. [PubMed: 11448902]
9. Shoba G, Joy D, Joseph T, Majeed M, Rajendran R, Srinivas PS. Influence of piperine on the pharmacokinetics of curcumin in animals and human volunteers. Planta Med 1998;64(4):353–353. [PubMed: 9619120]
10. Cheng AL, Hsu CH, Lin JK, Hsu MM, Ho YF, Shen TS, Ko JY, Lin JT, Lin BR, Ming-Shiang W, Yu HS, Jee SH, Chen GS, Chen TM, Chen CA, Lai MK, Pu YS, Pan MH, Wang YJ, Tsai CC, Hsieh CY. Phase I clinical trial of curcumin, a chemopreventive agent, in patients with high-risk or pre-malignant lesions. Anticancer Res 2001;21(4B):2895–900. [PubMed: 11712783]

11. Mahmmoud YA. Curcumin modulation of Na, K-ATPase: phosphoenzyme accumulation, decreased K+ occlusion, and inhibition of hydrolytic activity. Br J Pharmacol 2005;145(2):236–236. [PubMed: 15753945]
12. Bilmen JG, Khan SZ, Javed MH. Michelangeli FInhibition of the SERCA Ca2+ pumps by curcumin. Curcumin putatively stabilizes the interaction between the nucleotide-binding and phosphorylation domains in the absence of ATP. Eur J Biochem 2001;268(23):6318–6318. [PubMed: 11733029]
13. Egan ME, Pearson M, Weiner SA, Rajendran V, Rubin D, Glockner-Pagel J, Canny S, Du K, Lukacs GL, Caplan MJ. Curcumin, a major constituent of turmeric, corrects cystic fibrosis defects. Science 2004;304(5670):600–600. [PubMed: 15105504]
14. Zeitlin P. Can curcumin cure cystic fibrosis? N Engl J Med 2004;351(6):606–606. [PubMed: 15295056]
15. Wang W, Bernard K, Li G, Kirk KL. Curcumin opens CFTR channels by a novel mechanism that requires neither ATP binding NOR dimerization of the nucleotide binding domains. J Biol Chem. 2006
16. Loo TW, Bartlett MC, Clarke DM. Thapsigargin or curcumin does not promote maturation of processing mutants of the ABC transporters, CFTR, and P-glycoprotein. Biochem Biophys Res Commun 2004;325(2):580–580. [PubMed: 15530432]
17. Song Y, Sonawane ND, Salinas D, Qian L, Pedemonte N, Galietta LJ, Verkman AS. Evidence against the rescue of defective DeltaF508-CFTR cellular processing by curcumin in cell culture and mouse models. J Biol Chem 2004;279(39):40629–40629. [PubMed: 15280357]
18. Dragomir A, Bjorstad J, Hjelte L, Roomans GM. Curcumin does not stimulate cAMP-mediated chloride transport in cystic fibrosis airway epithelial cells. Biochem Biophys Res Commun 2004;322 (2):447–447. [PubMed: 15325250]
19. Grubb BR, Gabriel SE, Mengos A, Gentzsch M, Randell SH, Van Heeckeren AM, Knowles MR, Drumm ML, Riordan JR, Boucher RC. SERCA pump inhibitors do not correct biosynthetic arrest of deltaF508 CFTR in cystic fibrosis. Am J Respir Cell Mol Biol 2006;34(3):355–355. [PubMed: 16284361]
20. Kipp JE. The role of solid nanoparticle technology in the parenteral delivery of poorly water-soluble drugs. Int J Pharm 2004;284(1–2):109–22. [PubMed: 15454302]
21. Lao CD, Ruffin MTt, Normolle D, Heath DD, Murray SI, Bailey JM, Boggs ME, Crowell J, Rock CL, Brenner DE. Dose escalation of a curcuminoid formulation. BMC Complement Altern Med 2006;6:10. [PubMed: 16545122]
22. Anand P, Kunnumakkara AB, Newman RA, Aggarwal BB. Bioavailability of curcumin: problems and promises. Mol Pharm 2007;4(6):807–807. [PubMed: 17999464]
23. Soppimath KS, Aminabhavi TM, Kulkarni AR, Rudzinski WE. Biodegradable polymeric nanoparticles as drug delivery devices. J Control Release 2001;70(1–2):1–20. [PubMed: 11166403]
24. Desai MP, Labhasetwar V, Amidon GL, Levy RJ. Gastrointestinal uptake of biodegradable microparticles: effect of particle size. Pharm Res 1996;13(12):1838–1838. [PubMed: 8987081]
25. Hans ML, Lowman AM. Biodegradable nanoparticles for drug delivery and targeting. Current Opinion in Solid State and Materials Science 2002;6:319–327.
26. Middleton PG, Geddes DM, Alton EW. Protocols for in vivo measurement of the ion transport defects in cystic fibrosis nasal epithelium. Eur Respir J 1994;7(11):2050–2050. [PubMed: 7875281]
27. Southern, K.; Nasal, PD. University of Liverpool. 2001. [online]
28. Shankar TN, Shantha NV, Ramesh HP, Murthy IA, Murthy VS. Toxicity studies on turmeric (Curcuma longa): acute toxicity studies in rats, guineapigs & monkeys. Indian J Exp Biol 1980;18 (1):73–73. [PubMed: 6772551]
29. Panyam J, Labhasetwar V. Biodegradable nanoparticles for drug and gene delivery to cells and tissue. Adv Drug Deliv Rev 2003;55(3):329–329. [PubMed: 12628320]
30. Damge C, Maincent P, Ubrich N. Oral delivery of insulin associated to polymeric nanoparticles in diabetic rats. J Control Release 2007;117(2):163–163. [PubMed: 17141909]
31. Lin YH, Mi FL, Chen CT, Chang WC, Peng SF, Liang HF, Sung HW. Preparation and characterization of nanoparticles shelled with chitosan for oral insulin delivery. Biomacromolecules 2007;8(1):146–146. [PubMed: 17206800]

32. Grabovac V, Bernkop-Schnurch A. Development and in vitro evaluation of surface modified poly (lactide-co-glycolide) nanoparticles with chitosan-4-thiobutylamidine. Drug Dev Ind Pharm 2007;33 (7):767–767. [PubMed: 17654025]

33. Bisht S, Feldmann G, Soni S, Ravi R, Karikar C, Maitra A, Maitra A. Polymeric nanoparticle-encapsulated curcumin ("nanocurcumin"): a novel strategy for human cancer therapy. J Nanobiotechnology 2007;5:3. [PubMed: 17439648]

34. Win KY, Feng SS. Effects of particle size and surface coating on cellular uptake of polymeric nanoparticles for oral delivery of anticancer drugs. Biomaterials 2005;26(15):2713–2713. [PubMed: 15585275]

35. Thanos CG, Liu Z, Reineke J, Edwards E, Mathiowitz E. Improving relative bioavailability of dicumarol by reducing particle size and adding the adhesive poly(fumaric-co-sebacic) anhydride. Pharm Res 2003;20(7):1093–1093. [PubMed: 12880296]

36. Shakweh M, Besnard M, Nicolas V, Fattal E. Poly (lactide-co-glycolide) particles of different physicochemical properties and their uptake by peyer's patches in mice. Eur J Pharm Biopharm 2005;61(1–2):1–13. [PubMed: 16005619]

37. Kumar M, Bakowsky U, Lehr C. Preparation and characterization of cationic PLGA nanospheres as DNA carriers. Biomaterials 2004;25:1771–1777. [PubMed: 14738840]

38. Kwok, D. Discussion regarding detectable levels of curcumin in serum using the HPLC analystical method. BRI Biopharmaceutical Research Inc; Vancouver, BC: 2005.

39. Cartiera MS, Johnson KM, Rajendran V, Caplan MJ, Saltzman WM. The uptake and intracellular fate of PLGA nanoparticles in epithelial cells. Biomaterials 2009;30(14):2790–2790. [PubMed: 19232712]

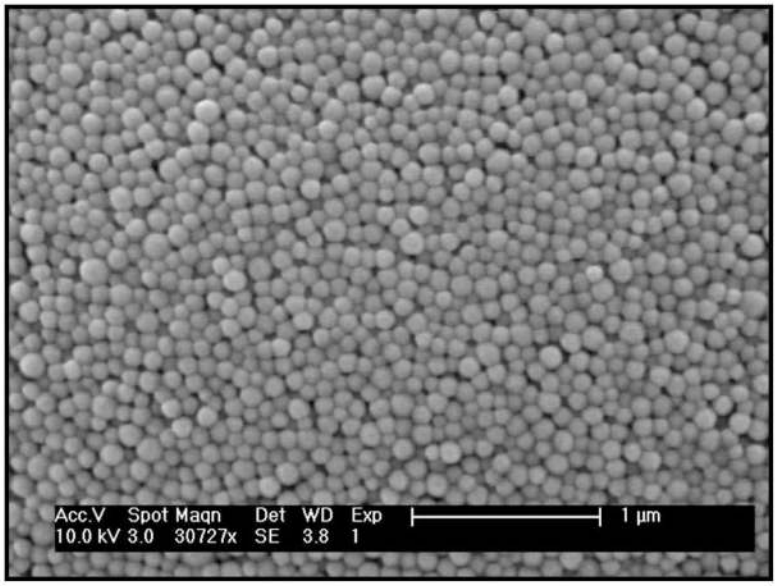

Figure 1.
Representative scanning electron micrograph of curcumin NPs. Image is presented at ~30,000x magnification. PLGA nanoparticles were prepared using a single emulsion method and resulted in a mean diameter of 77nm ± 16nm.

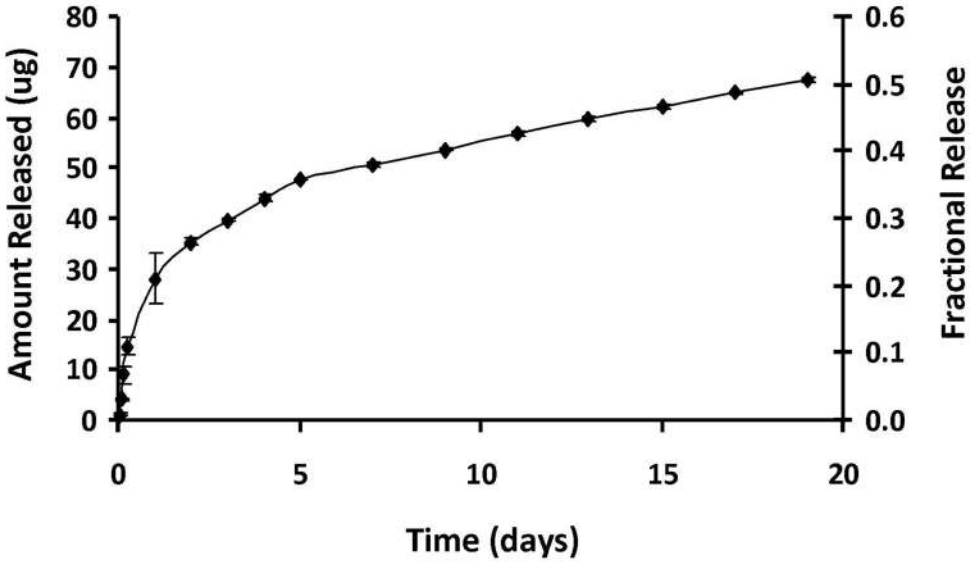

Figure 2.
Controlled-release profile for nanoparticles loaded with curcumin; 7.6% w/w loading. A biphasic profile is observed with an initial burst release during the first several hours followed by a sustained, more uniform release.

Figure 3a

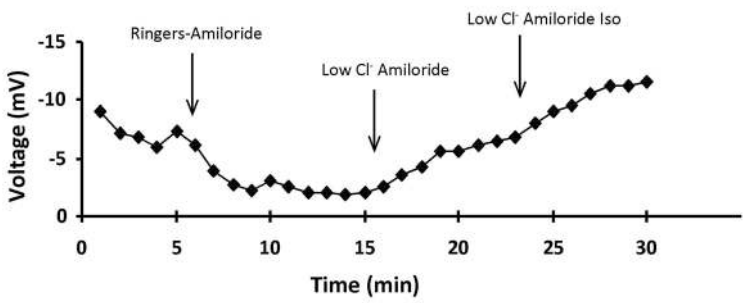

Figure 3b

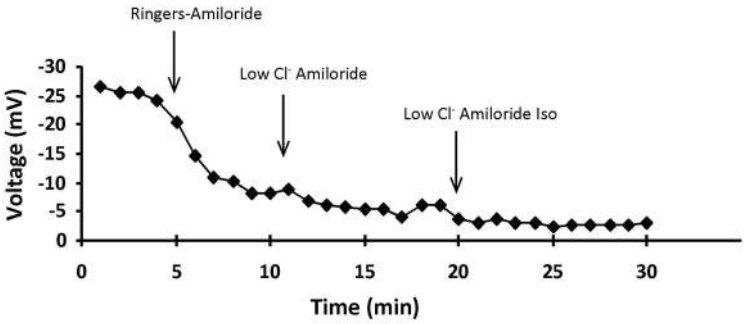

Figure 3.

Typical NPD traces for a heterozygote (a) and a cystic fibrosis affected (b) mouse. Arrows demarcate a solution change: Ringers → Ringers Amiloride → Low Chloride Amiloride → Low Chloride Isoproterenol. The most notable difference between the two groups is observed following administration of the β-agonist, Isoproterenol. In normal subjects isoproterenol elicits cAMP-regulated chloride secretion, however, this response is blunted or absent in CF-affected patients and animal models.

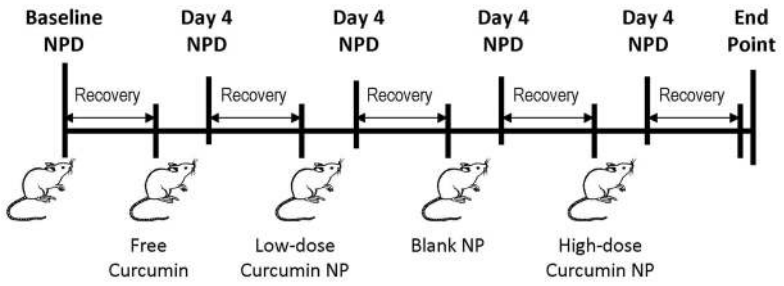

Figure 4.

Treatment dosing scheme. Individual baseline NPD measurements were taken prior to any treatment followed by oral administration of (1) free curcumin: total of 3.75 mg, (2) non-drug loaded NPs, (3) curcumin NPs at a low-dose: total curcumin encapsulated amount equivalent to 3.75 mg, and (4) curcumin NPs at a high-dose: curcumin amount released from nanoparticles at Day 4 equivalent to 3.75 mg. Mice were provided a 2 week recovery period between treatments to allow for clearance of anesthetic and effects associated with prior treatment.

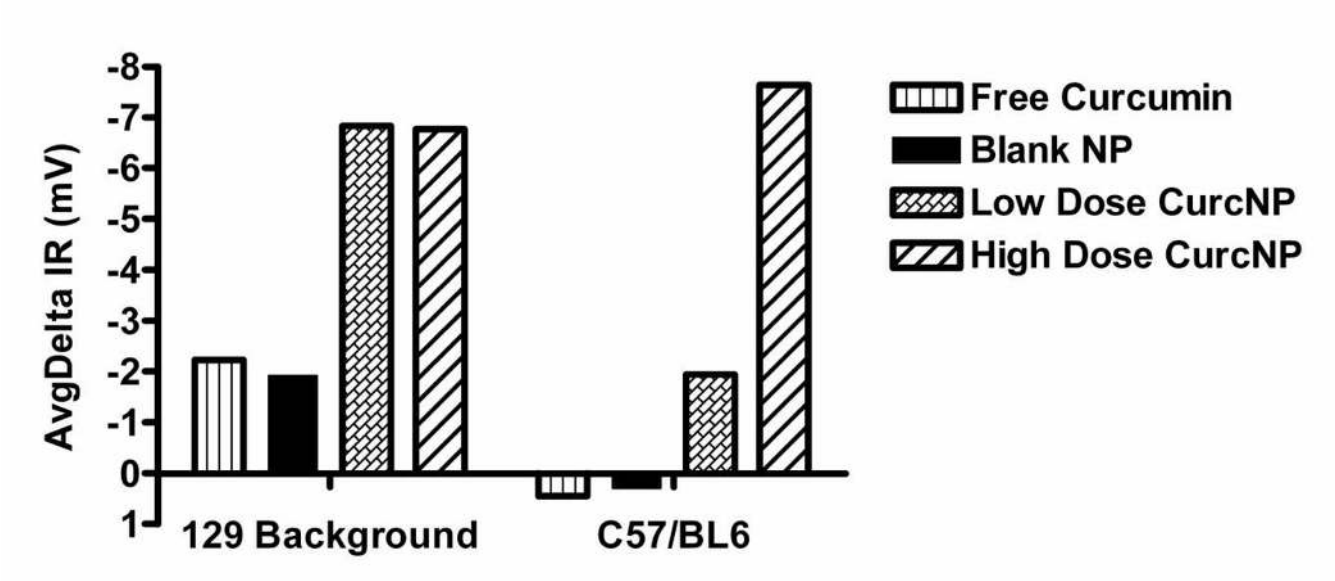

Figure 5.
Isoproterenol Response (IR) to specific treatments. Data shown is representative individual mouse data for subjects belonging to 129 background and C57/BL6 mouse strains.

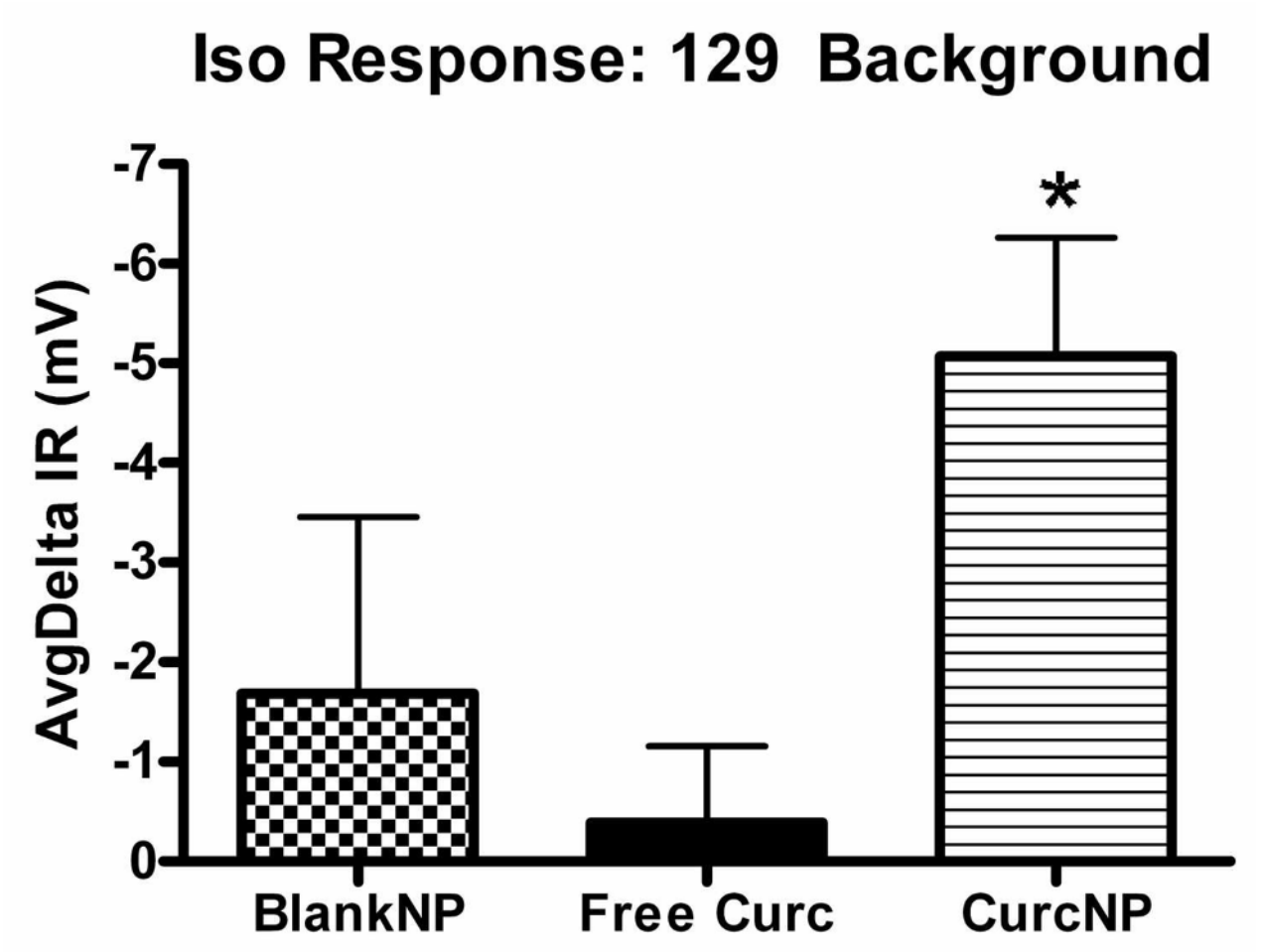

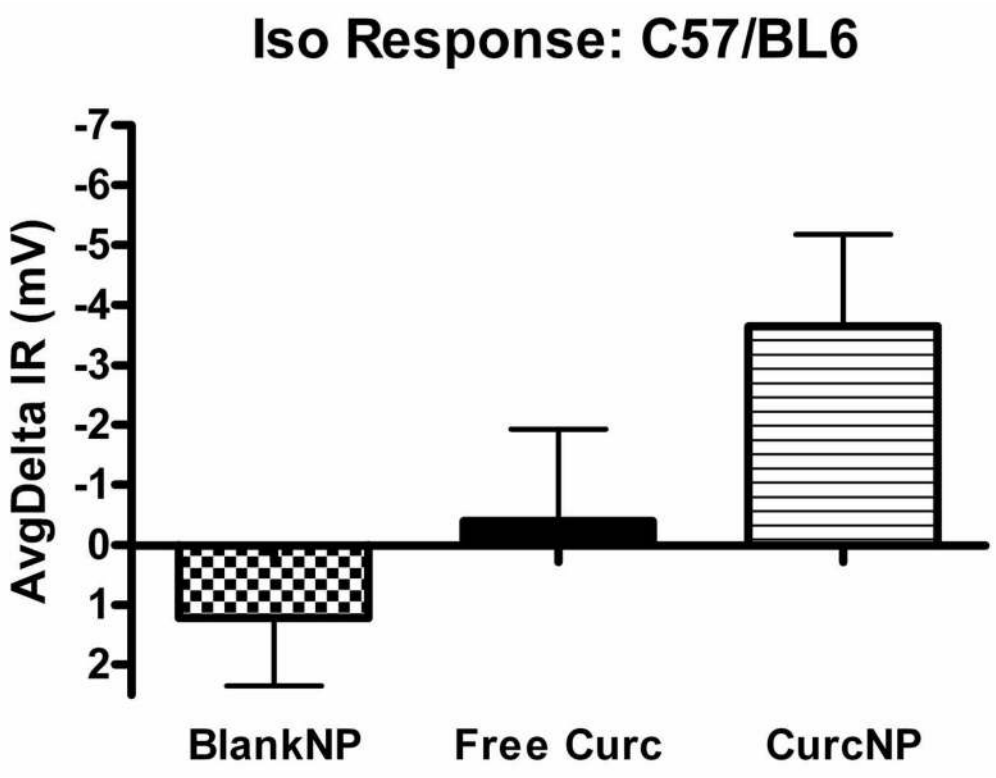

Figure 6.
Isoproterenol Response for 129 background (a) and C57/BL6 (b) mouse strains. Pooled NPD data was normalized to baseline and average response calculated for each group. Error bars represent ±SEM; *P < 0.05 compared to free curcumin treatment.

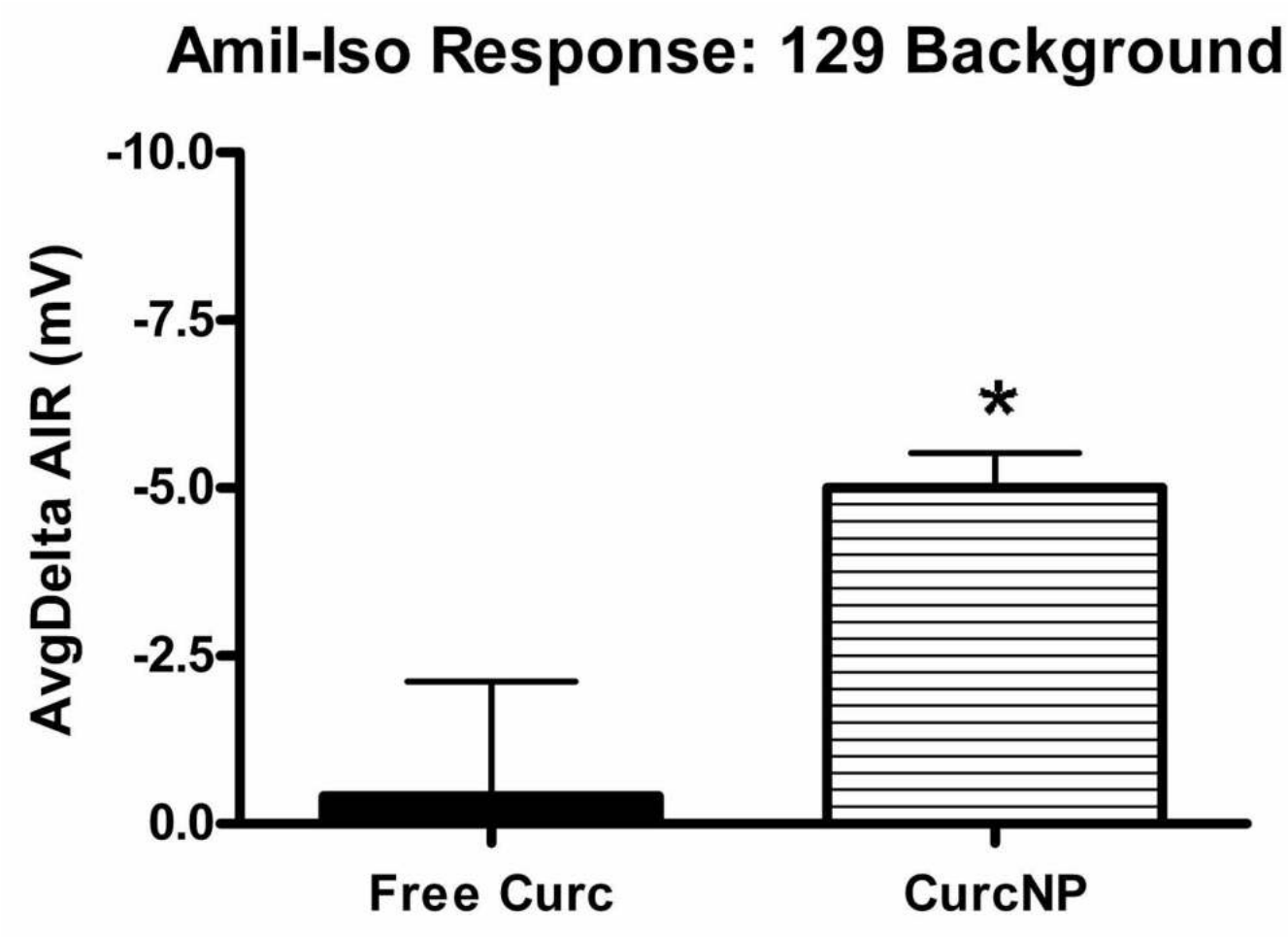

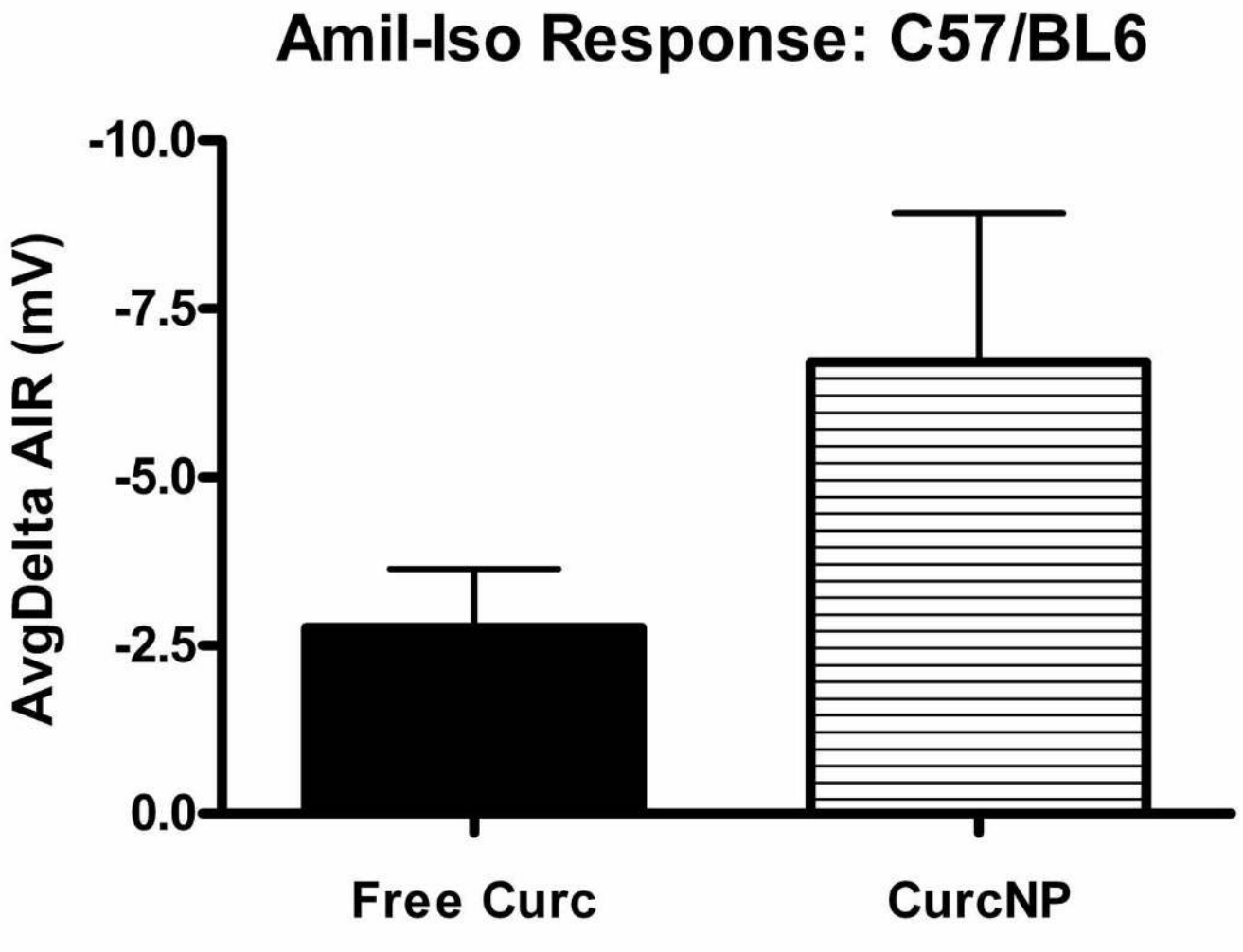

Figure 7.
Amiloride-Isoproterenol Response for 129 background (a) and C57/BL6 (b) mouse strains. Pooled NPD data was normalized to baseline and average response calculated for each group. Error bars represent ±SEM; *P < 0.05 compared to free curcumin treatment.

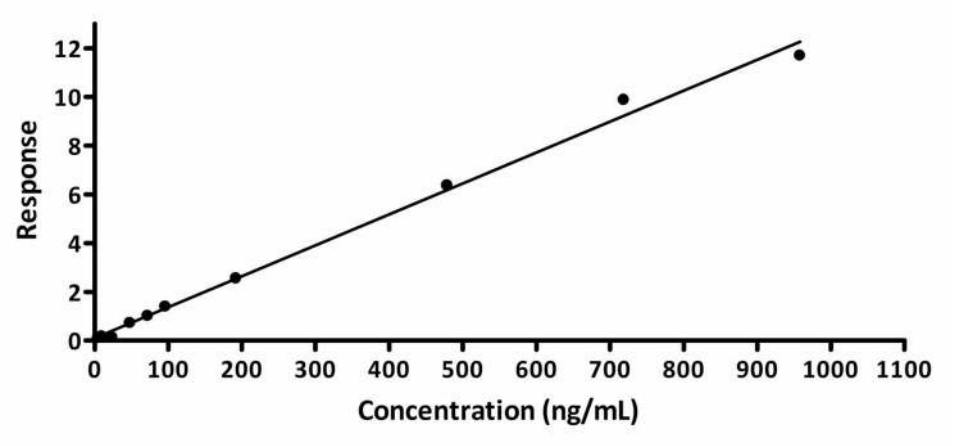

Figure 8.
Standard curve generated with curcumin-spiked mouse serum samples under optimized LC/MS/MS conditions.

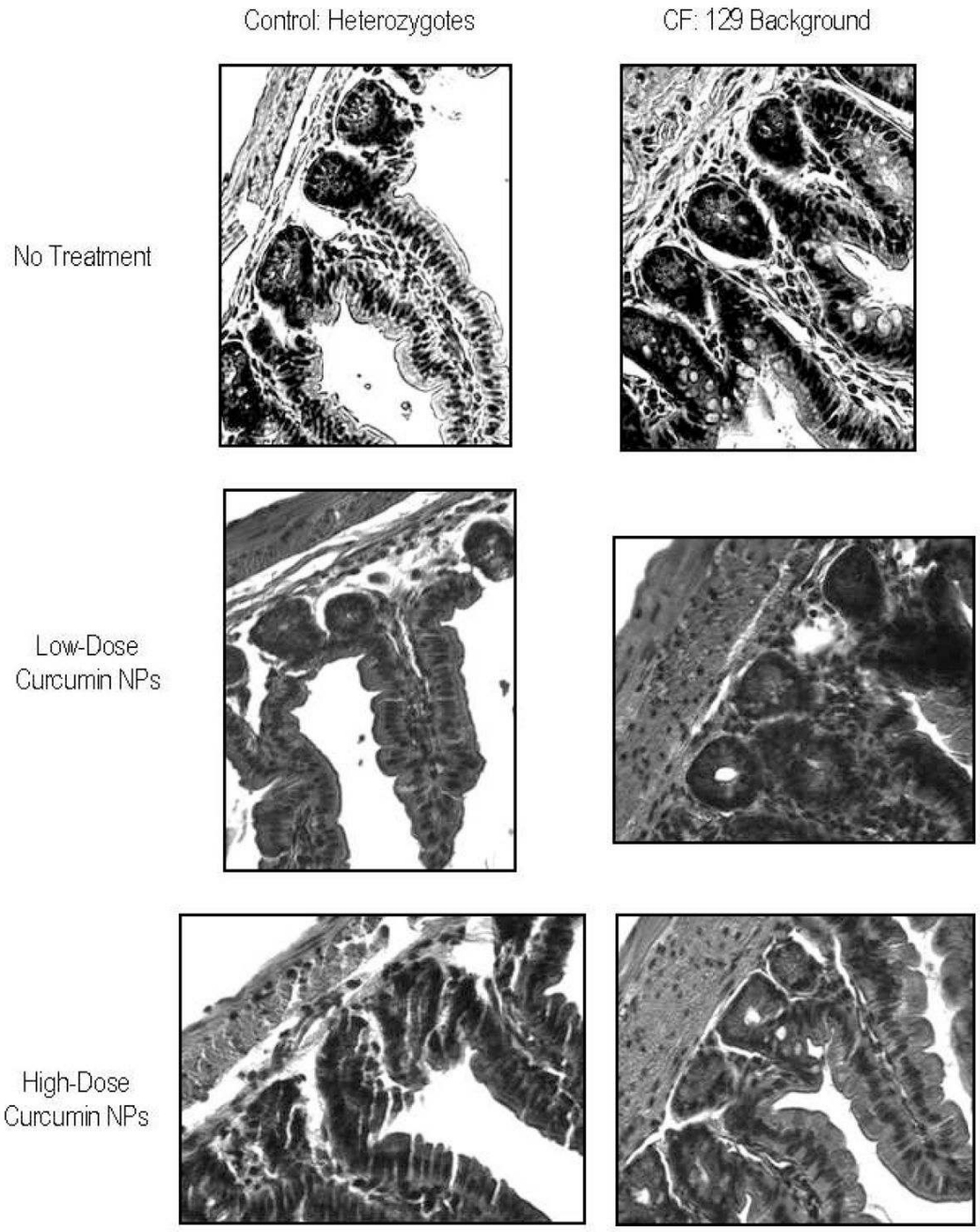

Figure 9.
Bright field images (60x) of hematoxylin and eosin stained, 5um thick ileum tissue slices from 129 background heterozygote mice (left) and CF mice (right). Representative images include the following groups: no treatment (top), treatment with a low-dose of curcumin NPs (middle), and treatment with a high-dose of curcumin NPs (bottom).